



Journal of Applied Pharmaceutical Research
Volume 6, Issue 2, Year of Publication 2018, Page 01 – 15
DOI: 10.18231/2348-0335.2018.0006



Research Article

JOURNAL OF APPLIED PHARMACEUTICAL RESEARCH | JOAPR

www.japtronline.com

ISSN: 2348 – 0335

SYNTHESIS AND BIOLOGICAL EVALUATION OF SOME HETEROCYCLIC COMPOUNDS

Menna-Allah Mohamed, Yassin Mohamed, Nahed M. Eid*, Flora F. Barsoum

Article Information

Received: 12th December 2017

Revised: 14th May 2018

Accepted: 30th May 2018

Keywords

Pyrrrole, pyrrolo[2,3-d]pyrimidine, anticancer, HepG2, MCF-7, VEGFR-2

ABSTRACT

Cancer is one of the most striking diseases that has a potential impact on human health with high mortality rate. During the last century many anticancer agents have emerged but unfortunately, these agents could not provide effective solutions for cancer treatment due to side effects and resistance. All over the world, asking for new anticancer agents is still a major goal for medicinal chemists. Pyrrole and pyrrolo[2,3-d]pyrimidine scaffolds are very interesting bioactive core exhibiting several biological activities as anticancer, anti-inflammatory, antimicrobial activities. Herein, we highlighted on the anticancer activity of the pyrrole and pyrrolo[2,3-d]pyrimidine derivatives which are reported to possess anticancer activity and many of them are in market or still in clinical trials. This work deals with design and synthesis of new pyrrole and pyrrolopyrimidine derivatives. The new compounds were screened for their cytotoxic activity against HepG2 and MCF7 *in vitro*. The most active compounds were evaluated for their VEGFR-2 inhibition *in vitro*

INTRODUCTION

Cancer is one of the most striking diseases that has a potential impact on human health with high mortality rate [1,2]. During the last century many anticancer agents have emerged but unfortunately, these agents could not provide effective solutions for cancer treatment due to side effects and resistance [1,3]. Therefore, asking for new anticancer agents is still a major goal for medicinal chemists all over the world. Among

many chemical scaffolds with anticancer activity, pyrrole and pyrimidine derivatives **I-VI** comprise a major class of several trials to develop new anticancer agents **Fig 1**. Their anticancer activity was achieved through inhibition of several enzymes [4-9]. Different novel pyrrole derivatives bearing sulfonamide moiety were reported to have promising activity against human liver cancer cell line (HepG2) and human breast cancer cell line (MCF-7) [10] through protein kinases inhibition [11]. Through

* Pharmaceutical Chemistry Department, Faculty of Pharmacy, Cairo University, Cairo, Egypt

*For Correspondence: n.elhabaly@yahoo.com

©2018 The authors

This is an Open Access article distributed under the terms of the Creative Commons Attribution (CC BY NC), which permits unrestricted use, distribution, and reproduction in any medium, as long as the original authors and source are cited. No permission is required from the authors or the publishers. (<https://creativecommons.org/licenses/by-nc/4.0/>)

the past few years, designing novel VEGFR-2 inhibitors have received great attention [12]. Among anti angiogenesis agents, VEGFR-2 inhibitors were used to control growth of tumors [13]. VEGFRs comprise a type of receptor tyrosine kinases (RTKs) which consist of single transmembrane domain that separates extracellular domain from intracellular tyrosine kinase region [14-18]. Based on fore-mentioned facts and as a trial to design and synthesize new anticancer agents with VEGFR-2 inhibitory activity, new substituted 5,7-diphenyl pyrrole and pyrrolo[2,3-*d*]pyrimidine derivatives were synthesized bearing carboxylic moiety as bioisostere to sulfonamide moiety in order to explore their cytotoxic activity as VEGFR-2 inhibiting action.

This rationale was based on the virtual activity of some 5,7-diphenyl pyrrolo[2,3-*d*]pyrimidine derivative with sulfonamide group rather than our bioisosteric carboxylic group [14]. Moreover, some amide derivatives with sulfonamide moiety were synthesized for comparing their antitumor activity with their carboxylic analogues. The cytotoxic activity against human liver cancer cell line HepG2 and human breast cancer cell line MCF-7 of all synthesized compounds were evaluated using doxorubicin and as reference standard. The inhibitory activity of most active four compounds against vascular endothelial growth factor receptor-2 (VEGFR-2) was evaluated.

MATERIALS & METHODS

2.1. Experimental

Melting points were determined on Electrothermal Stuart SMP3 digital melting point apparatus and were uncorrected. Elemental microanalyses were performed at the Regional Center for Mycology and Biotechnology, Al-Azhar University. Infrared spectra were determined (KBr) using Shimadzu Infrared spectrometer (IR-435) and FT-IR 1650 (Perkin Elmer), Faculty of Pharmacy, Cairo University. ¹H-NMR spectra were performed in DMSO-*d*₆ using Joel, 300 MHz NMR spectrometer, Faculty of Science, Cairo University and Bruker, 400 MHz NMR spectrometer, Microanalytical unit, Faculty of Pharmacy, Cairo University. ¹³C-NMR spectra were recorded using Bruker, 100 MHz NMR spectrometer, Microanalytical unit, Faculty of Pharmacy, Cairo University. Mass spectra were performed at the Regional Center for Mycology and Biotechnology, Al-Azhar University. Thin layer

chromatography was carried out on silica gel TLC plates with fluorescence indicator (F254).

2.1.1. 4-((2-Oxo-2-phenylethyl)amino)benzoic acid **1**

A mixture of *p*-amino benzoic acid (1.37 g, 0.01 mol) and phenacyl bromide (1.98 g, 0.01 mol) in absolute ethanol (10 ml) refluxed for 3 hours. The yielded solid was filtered, dried and crystallized from dioxane to give **1**. Yellow powder, yield 51%, melting point 220 °C (190°C reported [19]) IR: $\nu_{\max}/\text{cm}^{-1}$ 3356.14 (NH), 3051.39 (CH arom.), 2972.31 (CH aliph.), 2546.04 (OH), 1675, 1670.35 (2 C=O). ¹H NMR (DMSO-*d*₆) δ : 4.78 (s, 2H, CH₂), 6.69 (m, 3H, Ar-H + NH, D₂O exchangeable), 7.54-7.71 (m, 5H, Ar-H), 8.06 (d, 2H, Ar-H, *J* = 8.1 Hz), 12.10 (s, 1H, OH, D₂O exchangeable). ¹³C NMR (DMSO-*d*₆) δ : 50.0, 112.0 (2), 117.3, 128.4 (2), 128.8 (2), 131.3 (2), 134.1, 135.4, 152.5, 167.7 (COOH), 196.5 (C=O). Anal. Calculated. for C₁₅H₁₃NO₃ (255.27): C, 70.58; H, 5.13; N, 5.49. Found: C, 70.69; H, 5.17; N, 5.72. Ms (m/z, %): 255 (M⁺, 8.11)

2.1.2. 4-(2-Amino-3-cyano-4-phenyl-1H-pyrrol-1-yl)benzoic acid **2**

A mixture of **1** (2.55 g, 0.01 mol) and malononitrile (0.66 g, 0.01 mol) in absolute ethanol (30 ml) / sodium hydroxide (0.5 gm) refluxed for 12 hours. The reaction mixture cooled, poured on ice/water and acidified with dil. acetic acid. The obtained solid was crystallized from dioxane to give **2**. Orange brown powder, yield 89%, melting point 250 °C, IR: $\nu_{\max}/\text{cm}^{-1}$ 3402.43, 3338.78 (NH₂), 3057.17 (CH arom.), 2540 (OH), 2200.78 (CN), 1685.79 (C=O). ¹H NMR (DMSO-*d*₆) δ : 6.09 (s, 2H, NH₂, D₂O exchangeable), 6.96 (s, 1H, CH pyrrole), 7.23 (d, 2H, Ar-H, *J* = 8.9 Hz), 7.27-7.66 (m, 5H, Ar-H), 8.06 (d, 2H, Ar-H, *J* = 8.7 Hz), 13.00 (s, 1H, OH, D₂O exchangeable). ¹³C NMR (DMSO-*d*₆) δ : 71.3, 113.4 (C≡N), 118.3, 123.2, 125.1, 125.9 (2), 127.1, 129.7 (2), 130.7 (2), 131.2 (2), 133.5, 140.9, 148.7, 167.3 (COOH). Anal. Calcd. for C₁₈H₁₃N₃O₂ (303.31): C, 71.28; H, 4.32; N, 13.85. Found: C, 71.43; H, 4.30; N, 14.03. Ms (m/z, %): 303 (M⁺, 100).

2.1.3 4-(4-Amino-5-phenyl-7H-pyrrolo[2,3-*d*]pyrimidin-7-yl) benzoic acid **3**

A solution of **2** (3.03 g, 0.01 mol.) with formamide (30 ml) was refluxed for 10 hours. The reaction mixture was cooled, poured on ice/water and the solid obtained was crystallized from dioxane to give **3**. Black powder, yield 98%, melting

point 240 °C, IR: $\nu_{\max}/\text{cm}^{-1}$ 3304.06, 3167.12 (NH₂), 3061.03 (CH arom.), 2879.72 (OH), 1678.07 (C=O). ¹H NMR (DMSO-d₆) δ : 6.23 (s, 2H, NH₂, D₂O exchangeable), 7.38 (d, 2H, Ar-H, *J*= 9.0 Hz), 7.41-7.95 (m, 6H, Ar-H + CH pyrrole), 8.02 (d, 2H, Ar-H, *J*= 8.7 Hz), 8.26 (s, 1H, CH pyrimidine). ¹³C NMR (DMSO-d₆) δ : 101.7, 118.2, 123.0, 127.7, 129.1 (2), 129.5, 130.8, 132.1 (2), 134.4 (2), 140.3 (2), 150.8, 153.0, 158.1, 163.4, 167.6 (COOH). Anal. Calcd. for C₁₉H₁₄N₄O₂ (330.34): C, 69.08; H, 4.27; N, 16.96. Found: C, 69.24; H, 4.34; N, 17.15

2.1.4 4-(4-Oxo-5-phenyl-3,4-dihydro-7H-pyrrolo[2,3-d]pyrimidin-7-yl) benzoic acid **4**

A solution of **2** (3.03 g, 0.01 mol.) with formic acid (30 ml) was refluxed for 10 hours. The reaction mixture was cooled, poured on ice/water and the yielded solid was crystallized from ethanol to give **4**. Brown powder, yield 97%, melting point >300 °C, IR: $\nu_{\max}/\text{cm}^{-1}$ 3149.76 (NH), 3053.32 (CH arom.), 2550 (OH), 1685.79, 1654.92 (2 C=O). ¹H NMR (DMSO-d₆) δ : 7.24 (d, 2H, Ar-H, *J*= 8.9 Hz), 7.39-8.06 (m, 7H, Ar-H + CH pyrrole and CH pyrimidine), 8.09 (d, 2H, Ar-H, *J*= 8.9 Hz), 12.22 (s, 1H, NH, D₂O exchangeable), 12.96 (s, 1H, OH, D₂O exchangeable). ¹³C NMR (DMSO-d₆) δ : 107.0, 121.7, 121.9, 124.5, 126.9 (2), 128.8, 128.5 (2), 130.7 (2), 133.6 (2), 141.1, 145.2, 148.6, 158.8, 163.5 (C=O), 167.2 (COOH). Anal. Calcd. for C₁₉H₁₃N₃O₃ (331.32): C, 68.88; H, 3.95; N, 12.68. Found: C, 68.97; H, 4.07; N, 12.57. Ms (m/z, %): 331 (M⁺, 100).

2.1.5. 4-(4-Amino-2-oxo-5-phenyl-1,2-dihydro-7H-pyrrolo[2,3-d]pyrimidin-7-yl)benzoic acid **5**

A mixture of **2** (3.03 g, 0.01 mol.) and urea (0.6 g, 0.01 mol) fused at 220°C for 15 minutes on sand bath. The solid obtained was triturated with ethanol then filtered and crystallized from methanol to give **5**. Yellowish brown powder, yield 85%, melting point 210 °C, IR: $\nu_{\max}/\text{cm}^{-1}$ 3462.22, 3348.42, 3207.62 (NH, NH₂), 3062.96 (CH arom.), 2750 (OH), 1716.65, 1697.36 (2 C=O). ¹H NMR (DMSO-d₆) δ : 5.37 (s, 2H, NH₂, D₂O exchangeable), 7.39-7.98 (m, 10H, Ar-H + CH pyrrole), 8.04 (s, 1H, NH, D₂O exchangeable), 11.00 (s, 1H, OH, D₂O exchangeable). ¹³C NMR (DMSO-d₆) δ : 112.9, 117.0, 118.1, 119.1, 120.5 (2), 121.5, 122.8 (2), 128.4 (2), 129.0 (2), 130.5, 131.6, 150.4, 155.9 (C=O), 160.1, 167.6 (COOH). Anal. Calcd. for C₁₉H₁₄N₄O₃ (346.34): C, 65.89; H, 4.07; N, 16.18. Found: C, 66.03; H, 4.03; N, 16.39.

2.1.6. Synthesis of compounds **6** and **7**

A solution of **2** (3.03 g, 0.01 mol.) in acetic anhydride (30 ml) was refluxed for 15 minutes resulting in compound **6** and for 3 hours resulting in compound **7**. The reaction mixture was cooled, poured on ice/water while stirring and the yielded solid was crystallized from ethanol.

2.1.6.1.4-(2-Acetamido-3-cyano-4-phenyl-1H-pyrrol-1-yl) benzoic acid **6**

Brownish yellow powder, yield 75%, melting point 130 °C, IR: $\nu_{\max}/\text{cm}^{-1}$ 3223.05 (NH), 3062.96-3014.74 (CH arom.), 2536.39 (OH), 2223.92 (CN), 1695.43 (2 C=O). ¹H NMR (DMSO-d₆) δ : 1.97 (s, 3H, CH₃), 7.34-8.10 (m, 10H, Ar-H + CH pyrrole), 10.17 (s, 1H, NH, D₂O exchangeable), 13.00 (s, 1H, OH, D₂O exchangeable). ¹³C NMR (DMSO-d₆) δ : 25.8 (CH₃), 90.0, 115.8 (C≡N), 119.0, 121.2, 124.5, 124.9 (2), 126.4, 127.8 (2), 129.5 (2), 131.0 (2), 132.5, 134.5, 140.8, 167.0 (COOH), 170.7 (C=O). Anal. Calcd. for C₂₀H₁₅N₃O₃ (345.35): C, 69.56; H, 4.38; N, 12.17. Found: C, 69.74; H, 4.40; N, 12.40.

2.1.6.2.4-(2-(N-acetylacetamido)-3-cyano-4-phenyl-1H-pyrrol-1-yl) benzoic acid **7**

Brown powder, yield 60%, melting point 140 °C, IR: $\nu_{\max}/\text{cm}^{-1}$ 2225.85 (CN), 1811.16, 1745.58, 1705.07 (3 C=O). ¹H NMR (DMSO-d₆) δ : 1.90 (s, 3H, CH₃), 2.25 (s, 3H, CH₃), 7.47-7.77 (m, 5H, Ar-H), 7.37 (d, 2H, Ar-H, *J*= 9.0 Hz), 7.90 (s, 1H, CH pyrrole), 8.09 (d, 2H, Ar-H, *J*= 8.9 Hz), 12.80 (s, 1H, OH, D₂O exchangeable). ¹³C NMR (DMSO-d₆) δ : 25.7 (2CH₃), 91.8, 114.8 (C≡N), 119.0, 121.2, 125.7, 126.4 (2), 128.3, 129.5 (2), 131.5 (2), 131.9 (2), 133.8, 134.5, 139.6, 166.7 (COOH), 172.4 (2C=O). Anal. Calcd. for C₂₂H₁₇N₃O₄ (387.39): C, 68.21; H, 4.42; N, 10.85. Found: C, 68.33; H, 4.49; N, 10.97. Ms (m/z, %): 387 (M⁺, 12.96).

2.1.7. 4-(3-Cyano-4-phenyl-2-ureido-1H-pyrrol-1-yl)benzoic acid **8**

A mixture of **2** (3.03 g, 0.01 mol.) with urea (0.6 g, 0.01 mol) in absolute ethanol (30 ml) / sodium hydroxide (0.5 g) was refluxed for 12 hours. The reaction mixture was cooled, poured on ice/water and acidified with diluted acetic acid. The solid obtained was crystallized from dioxane to give **8**. Brown powder, yield 70%, melting point 233 °C, IR: $\nu_{\max}/\text{cm}^{-1}$ 3402.43, 3336.85, 3317.56 (NH, NH₂), 3061.03 (CH arom.), 2522.89 (OH), 2200.78 (CN), 1689.64 (2 C=O). ¹H NMR

(DMSO- d_6) δ : 6.01 (s, 2H, NH₂, D₂O exchangeable), 6.95 (s, 1H, CH pyrrole), 7.23 (d, 2H, Ar-H, J = 6.0 Hz), 7.28-7.66 (m, 6H, Ar-H + NH, D₂O exchangeable), 8.06 (d, 2H, Ar-H, J = 6.0 Hz). ¹³C NMR (DMSO- d_6) δ : 78.25, 112.0 (C \equiv N), 118.0, 122.9, 125.5, 126.5 (2), 127.8, 129.3 (2), 129.9 (2), 131.6 (2), 132.8, 141.3, 153.8, 162.8 (C=O), 167.1 (COOH). Anal. Calcd. for C₁₉H₁₄N₄O₃ (346.34): C, 65.89; H, 4.07; N, 16.18. Found: C, 66.04; H, 4.13; N, 16.34.

2.1.8. Synthesis of compounds 9-13

A mixture of **2** (3.03 g, 0.01 mol.) and the corresponding aromatic aldehyde (0.01 mol) in absolute ethanol (30 ml) was refluxed for 6 hours, concentrated and cooled. The yielded solid was crystallized from ethanol to give **9-13**, respectively.

2.1.8.1. 4-(2-(Benzylideneamino)-3-cyano-4-phenyl-1H-pyrrol-1-yl)benzoic acid **9** Yellow powder, yield 55%, melting point 263 °C, IR: $\nu_{\max}/\text{cm}^{-1}$ 3032.10 (CH arom.), 2665.62 (OH), 2214.28 (CN), 1691.57 (C=O). ¹H NMR (DMSO- d_6) δ : 7.37 (d, 2H, Ar-H, J = 6.0 Hz), 7.48-7.89 (m, 11H, Ar-H + CH pyrrole), 8.08 (d, 2H, Ar-H, J = 6.0 Hz), 9.14 (s, 1H, HC=N), 13.08 (s, 1H, OH, D₂O exchangeable). ¹³C NMR (DMSO- d_6) δ : 79.6, 117.5 (C \equiv N), 119.8, 125.8, 126.0, 126.7 (2), 128.0, 129.5 (2), 129.6 (2), 130.3 (2), 130.6 (2), 132.6 (2), 133.5, 135.5 (2), 141.0, 147.0, 163.6 (C=N), 167.0 (COOH). Anal. Calcd. for C₂₅H₁₇N₃O₂ (391.42): C, 76.71; H, 4.38; N, 10.74. Found: C, 76.87; H, 4.44; N, 10.88.

2.1.8.2. 4-(2-((4-Chlorobenzylidene)amino)-3-cyano-4-phenyl-1H-pyrrol-1-yl)benzoic acid **10**

Yellow powder, yield 60%, melting point >300 °C, IR: $\nu_{\max}/\text{cm}^{-1}$ 3030.17 (CH arom.), 2550 (OH), 2231.64 (CN), 1724.36 (C=O). ¹H NMR (DMSO- d_6) δ : 6.99 (s, 1H, CH pyrrole), 7.36 (d, 2H, Ar-H, J = 8.9 Hz), 7.46-7.89 (m, 9H, Ar-H), 8.07 (d, 2H, Ar-H, J = 8.9 Hz), 9.14 (s, 1H, HC=N), 13.05 (s, 1H, OH, D₂O exchangeable). ¹³C NMR (DMSO- d_6) δ : 79.8, 117.4 (C \equiv N), 120.0, 125.2, 125.9, 126.6 (2), 127.0 (2), 128.0, 129.4 (2), 130.0 (2), 130.6 (2), 131.1 (2), 131.2, 132.5, 134.4, 137.8, 146.5, 161.9 (C=N), 167.0 (COOH). Anal. Calcd. for C₂₅H₁₆ClN₃O₂ (425.87): C, 70.51; H, 3.79; N, 9.87. Found: C, 70.62; H, 3.84; N, 9.96.

2.1.8.3. 4-(3-Cyano-2-((4-methoxybenzylidene) amino)-4-phenyl-1H-pyrrol-1-yl)benzoic acid **11**

Orange powder, yield 60%, melting point 285 °C, IR: $\nu_{\max}/\text{cm}^{-1}$ 3014.74 (CH arom.), 2924.09 (CH aliph.), 2540 (OH),

2202.71 (CN), 1691.57 (C=O). ¹H NMR (DMSO- d_6) δ : 3.85 (s, 3H, CH₃), 7.08 (d, 2H, Ar-H, J = 8.7 Hz), 7.10-7.85 (m, 10H, Ar-H + CH pyrrole), 8.06 (d, 2H, Ar-H, J = 8.4 Hz), 9.04 (s, 1H, HC=N), 13.07 (s, 1H, OH, D₂O exchangeable). ¹³C NMR (DMSO- d_6) δ : 56.0 (CH₃), 79.0, 115.1 (C \equiv N), 117.7 (2), 119.2, 125.8, 126.6, 127.9 (2), 128.3, 129.5 (2), 130.1, 130.5 (2), 131.6(2), 132.6 (2), 141.1 (2), 147.5, 162.9 (C=N), 163.6, 167.0 (COOH). Anal. Calcd. for C₂₆H₁₉N₃O₃ (421.45): C, 74.10; H, 4.54; N, 9.97. Found: C, 74.22; H, 4.59; N, 10.09. Ms (m/z, %): 421 (M⁺, 100).

2.1.8.4. 4-(3-Cyano-2-((4-(dimethylamino) benzylidene) amino)-4-phenyl-1H-pyrrol-1-yl)benzoic acid **12**

Orange powder, yield 60%, melting point 278 °C, IR: $\nu_{\max}/\text{cm}^{-1}$ 3055.24 (CH arom.), 2550 (OH), 2214.28 (CN), 1712.79 (C=O). ¹H NMR (DMSO- d_6) δ : 3.03 (s, 6H, 2 CH₃), 6.77 (d, 2H, Ar-H, J = 9.0 Hz), 7.31-7.79 (m, 10H, Ar-H + CH pyrrole), 8.05 (d, 2H, Ar-H, J = 8.4 Hz), 8.88 (s, 1H, HC=N), 13.16 (s, 1H, OH, D₂O exchangeable). ¹³C NMR (DMSO- d_6) δ : 56.0 (2CH₃), 71.4, 111.5 (C \equiv N), 113.5 (2), 116.2, 118.2, 119.0, 123.1, 125.4 (2), 125.9 (2), 126.5, 127.1 (2), 127.9 (2), 129.4 (2), 130.0, 131.2, 141.1, 148.6, 163.0 (C=N), 167.0 (COOH). Anal. Calcd. for C₂₇H₂₂N₄O₂ (434.49): C, 74.64; H, 5.10; N, 12.89. Found: C, 74.72; H, 5.14; N, 13.12.

2.1.8.5. 4-(3-Cyano-2-((4-hydroxy-3-methoxybenzylidene) amino)-4-phenyl-1H-pyrrol-1-yl)benzoic acid **13**

Yellowish orange powder, yield 65%, melting point 168 °C, IR: $\nu_{\max}/\text{cm}^{-1}$ 3421.72 (OH phenolic), 3034.03 (CH arom.), 2540 (OH carboxylic), 2208.49 (CN), 1691.57 (C=O). ¹H NMR (DMSO- d_6) δ : 3.84 (s, 3H, CH₃), 6.91-8.06 (m, 9H, Ar-H + CH pyrrole), 7.25 (d, 2H, Ar-H, J = 9.0 Hz), 8.06 (d, 2H, Ar-H, J = 8.9 Hz), 8.96 (s, 1H, HC=N), 10.05 (s, 1H, OH phenolic, D₂O exchangeable), 13.03 (s, 1H, OH carboxylic, D₂O exchangeable). ¹³C NMR (DMSO- d_6) δ : 56.0 (CH₃), 71.4, 113.0 (C \equiv N), 113.5, 118.2 (2), 121.8, 123.1, 125.2 (2), 125.9, 127.0 (2), 129.0 (2), 130.4 (2), 131.0 (2), 131.6 (2), 133.6, 141.0, 148.8, 167.2 (C=N), 167.5 (COOH). Anal. Calcd. for C₂₆H₁₉N₃O₄ (437.45): C, 71.39; H, 4.38; N, 9.61. Found: C, 71.54; H, 4.42; N, 9.75.

2.1.9. Synthesis of compounds 14 and 15

A mixture of compound **2** (3.03 g, 0.01 mol.) with thionyl chloride was refluxed for 3 hours, the excess thionyl chloride was distilled out till dryness under reduced pressure. The

residue was refluxed with the corresponding sulfonamide (0.01 mol.) and 4 drops of pyridine in dry benzene (30 ml) for 6-8 hours. The reaction mixture was concentrated and cooled. The yielded solid was crystallized from methanol to give **14** and **15**.

2.1.9.1 4-(2-Amino-3-cyano-4-phenyl-1*H*-pyrrol-1-yl)-N-(4-sulfamoyl-phenyl)benzamide**14**

Brown powder, yield 74%, melting point 220 °C, IR: $\nu_{\max}/\text{cm}^{-1}$ 3342.64-3259.70 (NH, 2NH₂), 3070.68 (CH arom.), 2204.64 (CN), 1658.78 (C=O), 1321.24, 1157.29 (SO₂). ¹H NMR (DMSO-d₆) δ : 7.09-8.15 (m, 18H, Ar-H + CH pyrrole + NH₂, D₂O exchangeable + SO₂NH₂, D₂O exchangeable), 10.71 (s, 1H, NH, D₂O exchangeable). Anal. Calcd. for C₂₄H₁₉N₅O₃S (457.51): C, 63.01; H, 4.19; N, 15.31. Found: C, 63.19; H, 4.23; N, 15.47. Ms (m/z, %): 457 (M⁺, 2.59).

2.1.9.2. 4-(2-Amino-3-cyano-4-phenyl-1*H*-pyrrol-1-yl)-N-(4-(N-(5-methylisoxazol-3-yl)sulfamoyl)phenyl)benzamide**15**

Brown powder, yield 63%, melting point 220 °C, IR: $\nu_{\max}/\text{cm}^{-1}$ 3346.50-3209.55 (2NH, NH₂), 3068.75 (CH arom.), 2204.64 (CN), 1726.29 (C=O), 1319.31, 1165 (SO₂). ¹H NMR (DMSO-d₆) δ : 2.30 (s, 3H, CH₃), 6.13 (s, 1H, CH oxazole), 7.08-8.09 (m, 16H, Ar-H + CH pyrrole + NH₂, D₂O exchangeable), 10.73 (s, 1H, NH amide, D₂O exchangeable), 11.32 (s, H, SO₂NH, D₂O exchangeable). Anal. Calcd. for C₂₈H₂₂N₆O₄S (538.58): C, 62.44; H, 4.12; N, 15.60. Found: C, 62.57; H, 4.23; N, 15.84.

2.1.10. Synthesis of compounds **16,17**

A solution of **14**, **15** (4.58 g, 5.39 g respectively, 0.01 mol.) in formic acid (30 ml) was refluxed for 10 hours. The reaction mixture was cooled, poured on ice/water and the yielded solid was crystallized from methanol to give **16**, **17** respectively

2.1.10.1. 4-(4-Oxo-5-phenyl-3,4-dihydro-7*H*-pyrrolo[2,3-d]pyrimidin-7-yl)-N-(4-sulfamoylphenyl)benzamide**16**

Brown powder, yield 38%, melting point 240 °C, IR: $\nu_{\max}/\text{cm}^{-1}$ 3334.92-3261.63 (2NH, NH₂), 3064.89 (CH arom.), 2954.95 (CH aliph.), 1668.43, 1651.07 (2C=O), 1319.31, 1157.29 (SO₂). ¹H NMR (DMSO-d₆) δ : 7.08-8.14 (m, 17H, Ar-H + CH pyrrole + NH, D₂O exchangeable + SO₂NH₂, D₂O exchangeable), 8.36 (s, 1H, CH pyrimidine), 10.70 (s, 1H, NH, D₂O exchangeable). Anal. Calcd. for C₂₅H₁₉N₅O₄S (485.52): C, 61.85; H, 3.94; N, 14.42. Found: C, 62.02; H, 3.97; N, 14.60. Ms (m/z, %): 485 (M⁺, 5.19).

2.1.10.2. N-(4-(N-(5-methylisoxazol-3-yl)sulfamoyl)phenyl)-4-(4-oxo-5-phenyl-3,4-dihydro-7*H*-pyrrolo[2,3-d]pyrimidin-7-yl)benzamide**17**

Brown powder, yield 47.5%, melting point 265 °C, IR: $\nu_{\max}/\text{cm}^{-1}$ 3317.56-3246.20 (3NH), 3066.82 (CH arom.), 2954.95 (CH aliph.), 1670.35 (2C=O), 1319.31, 1165 (SO₂). ¹H NMR (DMSO-d₆) δ : 2.30 (s, 3H, CH₃), 6.14 (s, 1H, CH oxazole), 7.32-8.12 (m, 15H, Ar-H + CH pyrrole + NH, D₂O exchangeable), 8.35 (s, 1H, CH pyrimidine), 10.63 (s, 1H, NH amide, D₂O exchangeable), 11.36 (s, H, SO₂NH, D₂O exchangeable). Anal. Calcd. for C₂₉H₂₂N₆O₅S (566.59): C, 61.48; H, 3.91; N, 14.83. Found: C, 61.62; H, 3.97; N, 14.98.

2.1.11. Synthesis of compounds **18-24**

A mixture of **2** (3.03 g, 0.01 mol.) with the corresponding aromatic benzoyl chloride or sulfonyl chloride (0.01 mol) in dry benzene (30 ml), add 4 drops pyridine was refluxed for 6 hours. The reaction mixture was concentrated and cooled. The yielded solid was crystallized from ethanol to give **18-24**, respectively.

2.1.11.1. 4-(2-Benzamido-3-cyano-4-phenyl-1*H*-pyrrol-1-yl)benzoic acid **18**

Green powder, yield 44.6%, melting point 240 °C, IR: $\nu_{\max}/\text{cm}^{-1}$ 3336.85 (NH), 3062.96 (CH arom.), 2534.46 (OH), 2202.71 (CN), 1724.36, 1693.50 (2 C=O). ¹H NMR (DMSO-d₆) δ : 6.05 (s, 1H, NH, D₂O exchangeable), 6.96-8.13 (m, 15H, Ar-H + CH pyrrole), 13.10 (s, 1H, OH, D₂O exchangeable). Anal. Calcd. for C₂₅H₁₇N₃O₃ (407.42): C, 73.70; H, 4.21; N, 10.31. Found: C, 73.88; H, 4.26; N, 10.47.

2.1.11.2. 4-(2-(4-Chlorobenzamido)-3-cyano-4-phenyl-1*H*-pyrrol-1-yl)benzoic acid**19**

Green powder, yield 55%, melting point 190 °C, IR: $\nu_{\max}/\text{cm}^{-1}$ 3352.28 (NH), 3055.24 (CH arom.), 2553.75 (OH), 2202.71 (CN), 1693.50 (2 C=O). ¹H NMR (DMSO-d₆) δ : 6.05 (s, 1H, NH, D₂O exchangeable), 6.76-8.28 (m, 14H, Ar-H + CH pyrrole), 13.10 (s, 1H, OH, D₂O exchangeable). ¹³C NMR (DMSO-d₆) δ : 71.3, 113.5 (C≡N), 118.0, 123.1, 125.5, 125.9 (2), 127.0, 129.1 (2), 130.0 (2), 131.0 (2), 131.5 (2), 133.6 (2), 134.7, 138.2 (2), 141.1, 148.8, 166.9 (CONH), 167.1 (COOH). Anal. Calcd. for C₂₅H₁₆ClN₃O₃ (441.87): C, 67.96; H, 3.65; N, 9.51. Found: C, 68.09; H, 3.69; N, 9.62.

2.1.11.3. 4-(3-Cyano-2-(4-nitrobenzamido)-4-phenyl-1H-pyrrol-1-yl)benzoic acid **20**

Green powder, yield 32%, melting point 210 °C, IR: $\nu_{\max}/\text{cm}^{-1}$ 3336.85 (NH), 3062.96 (CH arom.), 2534.46 (OH), 2202.71 (CN), 1724.36, 1693.50 (2 C=O). ^1H NMR (DMSO- d_6) δ : 6.05 (s, 1H, NH, D₂O exchangeable), 6.75-8.31 (m, 14H, Ar-H + CH pyrrole), 13.10 (s, 1H, OH, D₂O exchangeable). Anal. Calcd. for C₂₅H₁₆N₄O₅ (452.43): C, 66.37; H, 3.56; N, 12.38. Found: C, 66.61; H, 3.60; N, 12.53.

2.1.11.4. 4-(3-Cyano-2-(2,4-dichlorobenzamido)-4-phenyl-1H-pyrrol-1-yl)benzoic acid **21**

Green powder, yield 38.2%, melting point 178-180 °C, IR: $\nu_{\max}/\text{cm}^{-1}$ 3336.85 (NH), 3066.82 (CH arom.), 2534.46 (OH), 2202.71 (CN), 1724.36, 1697.36 (2 C=O). ^1H NMR (DMSO- d_6) δ : 6.05 (s, 1H, NH, D₂O exchangeable), 6.75-8.28 (m, 13H, Ar-H + CH pyrrole), 13.00 (s, 1H, OH, D₂O exchangeable). Anal. Calculated. for C₂₅H₁₅Cl₂N₃O₃ (476.31): C, 63.04; H, 3.17; N, 8.82. Found: C, 63.17; H, 3.25; N, 8.9.

2.1.11.5. 4-(3-Cyano-4-phenyl-2-(phenylsulfonamido)-1H-pyrrol-1-yl)benzoic acid **22**

Green powder, yield 41%, melting point 114 °C, IR: $\nu_{\max}/\text{cm}^{-1}$ 3336.85 (NH), 3062.96 (CH arom.), 2538.32 (OH), 2202.71 (CN), 1693.50 (C=O), 1300.02, 1149.57 (SO₂). ^1H NMR (DMSO- d_6) δ : 6.06 (s, 1H, NH, D₂O exchangeable), 6.82-8.22 (m, 15H, Ar-H + CH pyrrole), 13.10 (s, 1H, OH, D₂O exchangeable). Anal. Calcd. for C₂₄H₁₇N₃O₄S (443.47): C, 65.00; H, 3.86; N, 9.48. Found: C, 65.17; H, 3.92; N, 9.62.

2.1.11.6. 4-(2-(4-Chlorophenylsulfonamido)-3-cyano-4-phenyl-1H-pyrrol-1-yl)benzoic acid **23**

Green powder, yield 44%, melting point 135 °C, IR: $\nu_{\max}/\text{cm}^{-1}$ 3340.71 (NH), 3093.98 (CH arom.), 2538.32 (OH), 2202.71 (CN), 1693.50 (C=O), 1327.03, 1157.29 (SO₂). ^1H NMR (DMSO- d_6) δ : 6.05 (s, 1H, NH, D₂O exchangeable), 6.75-8.13 (m, 14H, Ar-H + CH pyrrole), 13.06 (s, 1H, OH, D₂O exchangeable). ^{13}C NMR (DMSO- d_6) δ : 71.4, 113.5 (C \equiv N), 118.3, 123.1, 125.2, 125.9 (2), 127.0, 129.1 (2), 129.9 (4), 130.5 (2), 131.2 (2), 133.6, 139.5, 139.9 (2), 148.8, 167.1 (COOH). Anal. Calcd. for C₂₄H₁₆ClN₃O₄S (477.92): C, 60.32; H, 3.37; N, 8.79. Found: C, 60.49; H, 3.41; N, 8.96. Ms (m/z, %): 477 (M⁺, 0.71), 479 (M⁺², 0.38)

2.1.11.7. 4-(3-Cyano-2-(4-methylphenylsulfonamido)-4-phenyl-1H-pyrrol-1-yl)benzoic acid **24**

Green powder, yield 53%, melting point 220 °C, IR: $\nu_{\max}/\text{cm}^{-1}$ 3317.56 (NH), 3062.96 (CH arom.), 2542.18 (OH), 2202.71 (CN), 1689.64 (C=O), 1384.89, 1153.43 (SO₂). ^1H NMR (DMSO- d_6) δ : 2.36 (s, 3H, CH₃), 6.05 (s, 1H, NH, D₂O exchangeable), 6.76-8.13 (m, 14H, Ar-H + CH pyrrole), 13.10 (s, 1H, OH, D₂O exchangeable). Anal. Calcd. for C₂₅H₁₉N₃O₄S (457.50): C, 65.63; H, 4.19; N, 9.18. Found: C, 65.81; H, 4.23; N, 9.31.

2.2. Biological evaluation

2.2.1. In vitro cytotoxicity assay

Newly synthesized compounds **2-24** were subjected to *in vitro* cytotoxicity evaluation against both human liver HepG2 and human breast MCF-7 cancer cell lines. The anticancer screening was carried out at the Regional Center for Mycology & Biotechnology, Al-Azhar University, Cairo, Egypt using doxorubicin as reference standard following the previously reported MTT assay method [20]

2.2.1.1. MTT proliferation assay

The tested human carcinoma cell lines were obtained from the American Type Culture Collection (ATCC, Rockville, MD). The cells were grown on RPMI-1640 medium supplemented with 10% heat inactivated fetal calf serum, 1% L-glutamine and 50 $\mu\text{g}/\text{ml}$ gentamycin. The cells were maintained at 37°C in a humidified atmosphere with 5% CO₂ incubator (Shellab 2406, USA) and were subcultured 2-3 times a week.

For antitumor assays, the tumor cell lines were suspended in medium at concentration 5×10^4 cell/well in Corning[®] 96-well tissue culture plates and then incubated for 24 hours. Then the tested compounds were added into 96-well plates (six replicates) to achieve seven concentrations for each compound. Six vehicle controls with media or 0.5 % DMSO were running for each of the 96 well plate as a control.

After incubating for 24 hours, the numbers of viable cells were determined by the MTT test. Briefly, the media was removed from the 96 well plate and replaced with 100 μl fresh culture RPMI 1640 medium without phenol red then 10 μl of the 12 mM MTT (Sigma) stock solution (5 mg of MTT in 1 mL of PBS) to each well including the untreated controls. The 96 well plates were then incubated at 37°C and 5% CO₂ for 4 hours.

An 85 µl aliquot of the media was removed from the wells and 50 µl of DMSO was added to each well and mixed thoroughly with the pipette and incubated at 37°C for 10 minutes. Then, the optical density was measured at 590 nm with the microplate reader (SunRise, TECAN, Inc, USA) to determine the number of viable cells.

2.2.1.2 VEGFR-2 inhibition in human liver cancer cell line HepG-2

In a trial to explore the mechanism of action of the most active compounds **5,9,12** and **13**, they were subjected to *in vitro* evaluation of their VEGFR-2 inhibition activity on HepG2 cell line using the human VEGFR2/KDR ELISA kit and percentage inhibition was calculated and compared with that of doxorubicin. It was carried out at VACSERA, Cairo, Egypt. Cell Line HepG2 was obtained from American Type Culture Collection. HepG2 cells were cultured using Dulbecco's Modified Eagle's medium (DMEM), supplemented with 10% fetal bovine serum (FBS), 10 µg/ml of insulin and 1% penicillin-streptomycin.

The cells (cells density 1.2 –1.8 ×10,000 cells/well) were cultured in a volume of 100µl complete growth medium, treated with 100 µl of IC₅₀ value of the tested compounds or the standard reference drug per well in 96-well plate and incubated for 24 hours. The cells were harvested and homogenates were prepared in saline using a tight pestle homogenizer until complete cell distribution [21]. The kit used a double-antibody sandwich enzyme-linked immunosorbent assay (ELISA) to assay the level of human VEGFR-2 in samples. An anti-human VEGFR2/KDR coating antibody is adsorbed on microwells. Human VEGFR2/KDR present in the sample or standard bound to antibodies adsorbed to the microwells.

A biotin-conjugated anti-human VEGFR2/KDR antibody was added and bound to human VEGFR2/KDR captured by the first antibody. Following incubation unbound biotin-conjugated anti-human VEGFR2/KDR antibody was removed during a wash step. Streptavidin-HRP was added and bound to the biotin-conjugated anti-human VEGFR2/KDR antibody. Then unbound Streptavidin-HRP was removed during a wash step and tetramethyl-benzidine (TMB) substrate solution reactive with HRP was added to the wells. A coloured product was formed in proportion to the amount of human VEGFR2/KDR present in the sample or standard. The reaction was terminated

by addition of acid and absorbance was measured at 450 nm. A standard curve was prepared from 7 human VEGFR2/KDR standard dilutions and then human VEGFR2/KDR level in sample was calculated (pg/ml).

2.2.2. Molecular docking

The docking process includes the prediction of ligand conformation and orientation within a targeted binding site, and the possible ligand-protein interactions. In general, docking aims at accurate structural modeling of the new hits and correct prediction of the activity [22]. The most active four compounds **5, 9, 12** and **13** were subjected to the molecular docking to reveal the inhibition type of them. To perform accurate validation of the docking protocol, docking of the co-crystallized ligand [sunitinib (type I inhibitor) (PDB: 4AGD), sorafenib (type II inhibitor) (PDB: 4ASD) or the co-crystallized ligand 99 (type III inhibitor) (PDB: 3VHK) should be carried out to study the scoring energy (S), root mean standard deviation (rmsd) and amino acid interactions. All docking procedures were achieved by MOE (Molecular Operating Environment) software 10.2008 provided by chemical computing group, Canada. Docking was performed using London dG force and refinement of the results was done using force field energy. The docking indicates that sunitinib is fitted in the active site pocket with S= -27.4945 Kcal/mol and rmsd= 1.4790, sorafenib is fitted in the active site pocket with S= -31.0703 Kcal/mol and rmsd= 0.7244. Docking of the most active compounds **5, 9, 12** and **13** in the active site of (PDB: 4AGD) and (PDB: 4ASD) did not succeed to show fitting in the active site and considered as failure of the compounds to interact with these active sites.

On the other hand, the ligand 99 is fitted in the active site pocket with S= -12.4340 Kcal/mol and rmsd= 0.9272. The same amino acid interactions were recognized with the hydrogen bonds previously mentioned. In this case the four compounds showed good fitting with a comparable manner to the co-crystallized ligand.

RESULTS & DISCUSSIONS

3.1. Chemistry

Reaction of 4-substituted amino benzoic acid **1** [19,23-24] with malononitrile in refluxing ethanolic sodium ethoxide solution afforded 4-(2-amino-3-cyano-4-phenyl-1H-pyrrol-1-yl)benzoic acid **2** [23-25].

Scheme 1 Reactions of compound **2** with formamide and formic acid afforded the derivatives **3, 4** respectively [25-29].

Scheme 2 The structure of compound **3** was confirmed by ^1H NMR spectrum spectral data showed two singlet signals at 7.83 and 8.26 ppm for 2 CH of pyrrole and pyrimidine rings, respectively and a singlet signal at 6.23 ppm for NH_2 group disappeared upon deuteration. ^1H NMR spectral data of compound **4** showed a singlet signal at 12.22 ppm attributed to the pyrimidine NH proton disappeared upon deuteration and singlet signal at 8.06 ppm assigned for CH proton of the pyrimidine ring. ^{13}C NMR spectrum showed presence of two signals at 163.5, 167.2 ppm for two C=O groups and COOH, respectively. Fusion of **2** with urea at 220°C created the oxopyrrolopyrimidine derivative **5** [2,27], while reaction of **2** with urea in ethanol in presence of sodium hydroxide gave the ureido-pyrrole derivative **8** [10, 30].

Scheme 2 ^1H NMR spectrum of compound **5** showed two singlet signals at 5.37 and 8.04 ppm for NH_2 and NH groups, respectively, which were exchangeable upon deuteration. ^{13}C NMR spectrum showed the presence of two signals at 155.9, 167.6 ppm for two carbonyl groups C=O and COOH, respectively. On the other hand, IR spectrum of compound **8** showed the appearance of the band corresponding to cyano group at 2200.78 cm^{-1} . ^1H NMR spectrum showed a singlet signal at 6.01 ppm for NH_2 group disappeared upon deuteration and a singlet signal at 6.95 for CH of pyrrole. Refluxing **2** with acetic anhydride for 15 minutes afforded the monoacetylate derivative **6**, while continue refluxing for 3 hours, diacetylation took place, compound **7** [25, 30].

Scheme 2 Compound **6** ^1H NMR spectrum displayed sharp singlet signal at 1.97 ppm representing the three protons of the CH_3 group, in addition to a broad singlet at 10.17 ppm attributed to NH group, which disappeared upon deuterium exchange. ^{13}C NMR spectrum revealed a signal at 25.8 ppm for CH_3 group IR spectrum of compound **7** showed the appearance of three bands at 1811.16, 1745.58 and 1705.07 cm^{-1} corresponding to the three carbonyl groups 2C=O and COOH, respectively. ^1H NMR spectrum showed two singlet signals at 1.90 and 2.25 ppm for 2 CH_3 group. Some Schiff's bases **9-13** prepared by refluxing different substituted aromatic aldehydes with **2** in absolute ethanol [31-33].

Scheme 3 IR spectra of compounds **9-13** revealed the appearance of cyano group bands at $2231.64 - 2202.71\text{ cm}^{-1}$. ^1H NMR spectra revealed the azomethine proton as sharp singlet signal at 8.88 - 9.14 ppm, with the disappearance of the amino protons singlet signal. The 2-amino-3-cyano-pyrrole derivative **2** was treated with thionyl chloride [35-36] to produce acid chloride intermediate which was immediately reacted with sulfanilamide or sulfamethoxazole in dry benzene, in the presence of few drops of pyridine [2,29,31] to produce the corresponding amide derivatives **14 and 15**, refluxing of the later compounds with formic acid yielded the corresponding pyrrolo[2,3-*d*]pyrimidine derivatives **16 and 17** [26-29, 36-37].

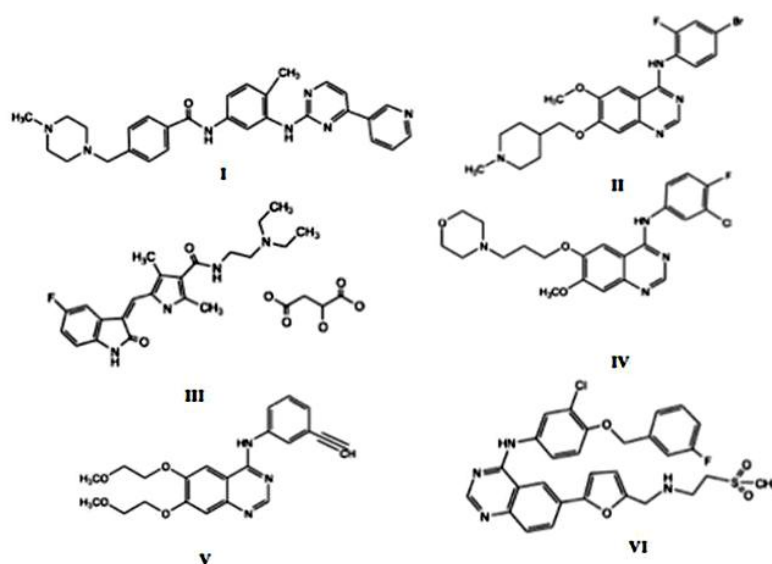
Scheme 4 IR spectra of **14 and 15** showed appearance of bands at $3346.50-3209.55\text{ cm}^{-1}$ for NH and NH_2 groups in addition to two bands at $1321.24, 1319.31\text{ cm}^{-1}$ and $1157.29, 1165\text{ cm}^{-1}$ assignable for the SO_2 group. ^1H NMR spectra revealed the appearance of singlet signals attributed to the amino protons of the sulfonamide moiety at 7.96 and 11.32 ppm, respectively, which were exchangeable upon deuteration. On the other hand, The IR spectra of **16 and 17** revealed two bands at $1670.35-1651.07\text{ cm}^{-1}$ attributed to the two carbonyl groups and at 2204.64 cm^{-1} for the nitrile group. ^1H NMR spectra exhibited the appearance of a singlet signal at 8.36 and 8.35, for CH proton of the pyrimidine ring. Refluxing **2** with different aromatic benzoyl chloride or sulfonyl chloride in dry benzene and few drops of pyridine afforded the benzamido- **18-21** and phenylsulfonamido-pyrrole derivatives **22-24** [2, 28, 30]

Scheme 5 IR spectra revealed two bands attributed to the two carbonyl groups at $1724.63- 1693.50\text{ cm}^{-1}$ for compounds **18-21** and the appearance of SO_2 bands at $1384.89-1300.02\text{ cm}^{-1}$ and $1157.29-1149.57\text{ cm}^{-1}$ for compounds **22-24**. ^{13}C NMR spectrum of compound **19** revealed two signals at 166.9 and 167.1 ppm for the two carbonyl groups of CONH and COOH, respectively, while compound **23** spectrum showed only one signal at 167.1 ppm for COOH.

3.2. Biological evaluation

3.2.1. In vitro cytotoxicity assay

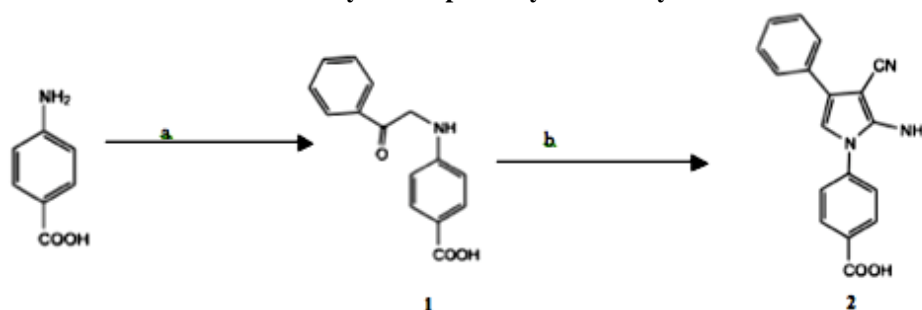
All the newly synthesized compounds **2-24** were evaluated for their cytotoxic activity against human breast MCF-7 and human liver HepG2 cancer cell lines using doxorubicin as reference standard following the previously reported MTT assay method [20].



I: Imatinib, II: Vandetanib, III: Sunitinib, IV: Gefitinib, V: Erlotinib, VI: Lapatinib

Figure 1: some pyrrole and pyrimidine derivatives have anticancer activity

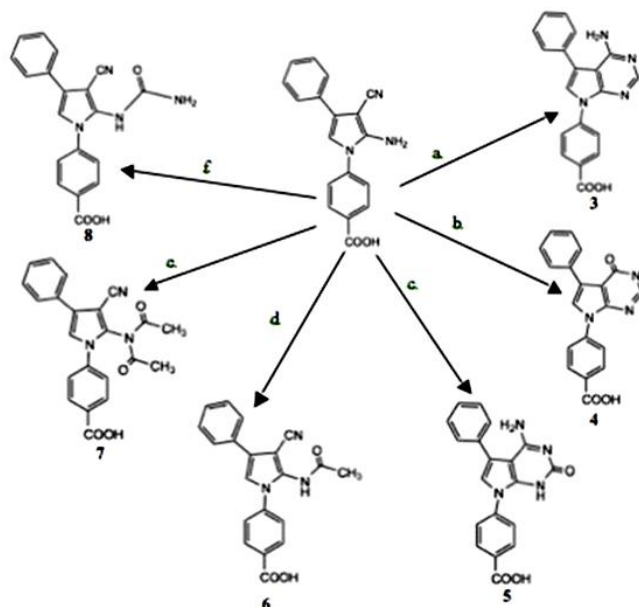
Scheme:1. Synthetic pathways of the key intermediate 2



Reagents and conditions: a) Phenacyl bromide, abs. ethanol, Reflux 3h;

b) Sodium ethoxide/ malononitrile, abs. ethanol, reflux 12h

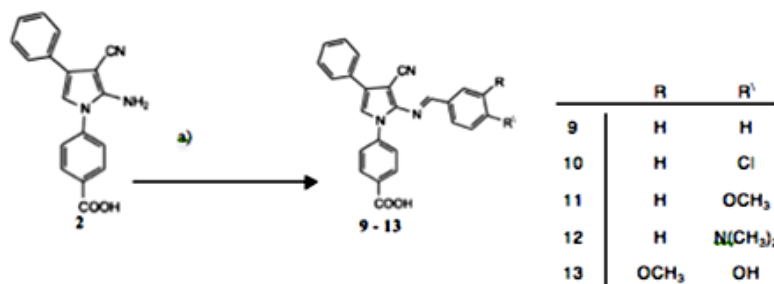
Scheme: 2 Synthetic pathways of the compounds 3-8



Reagents and conditions: a) formamide, reflux 10h; b) formic acid, reflux 10h; c) urea, fused at 15min.

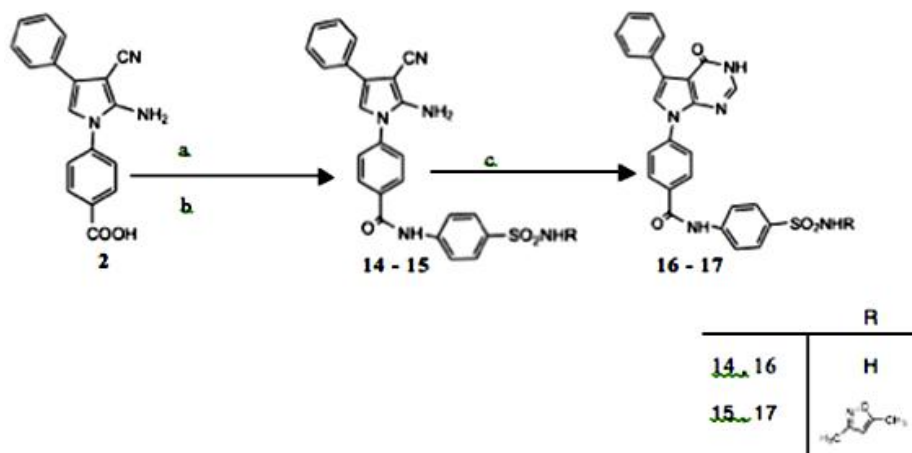
d) acetic anhydride, reflux 13min; e) acetic anhydride, reflux 3h; f) urea/sodium hydroxide, reflux 12h

Scheme: 3 General synthetic pathway of the compounds 9-13

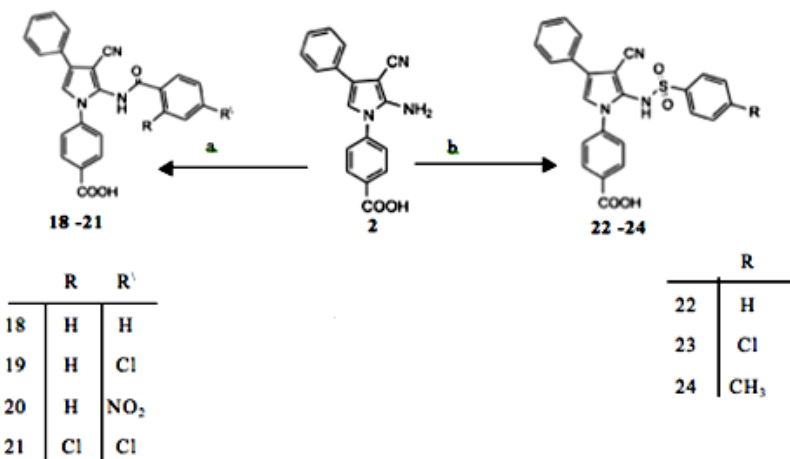


Reagents and conditions: a) aromatic aldehydes, abs. ethanol, reflux 6h

Scheme: 4 General synthetic pathways of the compounds 14-17



Reagents and conditions: a) thionyl chloride, reflux 3h; b) sulfonamides, pyridine, benzene, reflux 6-8h; c) formic acid, reflux 10h



Reagents and conditions: a) aryl benzoyl chloride, benzene, reflux 6h; b) aryl sulfonyl chloride, benzene, reflux 6h

The results are mean of three separated experiments \pm S.E. **Table 1** Pyrrolederivatives **6-15** and **18-24**; The acetyl substituent of the amino pyrrole **6** and **7**, respectively, showed a good activity against HepG2 with approximately the same IC₅₀ values (3.85 \pm 0.30 and 3.81 \pm 0.3 μ M, respectively). On the other hand, the ureido derivative **8** was the least active one (IC₅₀ = 13.59 \pm 1.2 μ M). These compounds were inactive against human breast MCF-7 (IC₅₀ > 50 μ m). Regarding the effect of

substituent on schiff's base, the unsubstituted derivative **9** and the vanillin derivative **13** had a good activity against HepG2 (IC₅₀ = 1.87 \pm 0.12 μ M). While the *p*-N, N-dimethyl derivative **12** showed nearly the same activity (IC₅₀ = 1.78 \pm 0.10 μ M). On the other hand, the *p*-methoxysubstituent **11** had a moderate activity (IC₅₀ = 4.79 \pm 0.3 μ M), while the *p*-chlorosubstituent **10** had the least activity against HepG2 (IC₅₀ = 12.51 \pm 1.1 μ M). Although the activity of these compounds against MCF-7 was

very weak, by comparing their activity, compounds **12** and **13** were the most active ones ($IC_{50} = 19.25 \pm 0.47$ and $23.12 \pm 1.25 \mu M$, respectively).

Table 1: IC_{50} of the newly synthesized compounds against HepG2 and MCF-7

compound	HepG2 $IC_{50} \pm S.E. (\mu M)$	MCF-7 $IC_{50} \pm S.E. (\mu M)$
2	40.7 \pm 8.3	49.21.8
3	3.29 \pm 0.25	>50
4	3.38 \pm 0.28	>50
5	1.91 \pm 0.10	>50
6	3.85 \pm 0.30	>50
7	3.81 \pm 0.35	>50
8	13.59 \pm 1.2	>50
9	1.87 \pm 0.13	40.89 \pm 1.5
10	12.51 \pm 1.1	>50
11	4.79 \pm 0.3	>50
12	1.78 \pm 0.10	19.25 \pm 0.47
13	1.87 \pm 0.12	23.12 \pm 1.25
14	>50	>50
15	>50	>50
16	>50	>50
17	>50	>50
18	41.2 \pm 1.4	19.2 \pm 0.5
19	>50	>50
20	>50	>50
21	>50	>50
22	9.13 \pm 0.2	40.2 \pm 1.4
23	>50	>50
24	7.35 \pm 0.2	>50
Doxorubicin	1.13 \pm 0.10	1.49 \pm 0.023

IC_{50} was obtained from three separated experiments \pm S.E.

On the other hand, compound **9** was less active ($IC_{50} = 40.89 \pm 1.5 \mu M$) and compounds **10** and **11** were inactive ($IC_{50} > 50 \mu M$). In this series, compound **12** was considered the most active one against both HepG2 and MCF-7 cell lines.

Converting the carboxylic moiety into the corresponding amide derivatives using sulfanilamide **14** and sulfamethoxazole **15** led to inactive derivatives ($IC_{50} > 50 \mu M$) against both HepG2 and MCF-7. Within phenylsulfonamido series **22-24**, the *p*-methyl phenylsulfonamide derivative **24** was the most active compound against HepG2 ($IC_{50} = 7.35 \pm 0.2 \mu M$), while the unsubstituted analogue **22** showed a moderate activity ($IC_{50} = 9.13 \pm 0.2 \mu M$). On the other hand, the *p*-chloro derivative **23** was inactive ($IC_{50} > 50 \mu M$).

Table 2: VEGFR 2 percentage inhibition

Compound	VEGFR 2 residual conc.	VEGFR-2 % inhibition
5	686.491	85.3
9	740.914	84.1
12	775.862	83.4
13	590.541	87.3
Doxorubicin	978.443	79.0

In case of benzamido derivatives **18-21**, all compounds were inactive ($IC_{50} > 50 \mu M$) except the unsubstituted derivative **18** which had a weak activity ($IC_{50} = 41.2 \pm 1.4 \mu M$). All the compounds **18-24** were inactive against MCF-7 ($IC_{50} > 50 \mu M$) except for **18** and **22** which exhibited a moderate to weak activity ($IC_{50} = 19.2 \pm 0.5$ and $40.2 \pm 1.4 \mu M$, respectively). Pyrrolopyrimidine derivatives **3-5** and **16,17**; The 4-amino, 2-oxo-pyrrolopyrimidine derivative **5** was the most active compound in this series against HepG2 ($IC_{50} = 1.91 \pm 0.10 \mu M$), while both the 4-amino derivative **3** and the 4-oxo derivative **4** showed lower activity ($IC_{50} = 3.29 \pm 0.25$ and $3.38 \pm 0.28 \mu M$, respectively). On the other hand, these compounds were inactive against MCF-7 cell line ($IC_{50} > 50 \mu M$). The sulfonamide pyrrolopyrimidine derivatives **16** and **17** were inactive ($IC_{50} > 50 \mu M$) against both HepG2 and MCF-7.

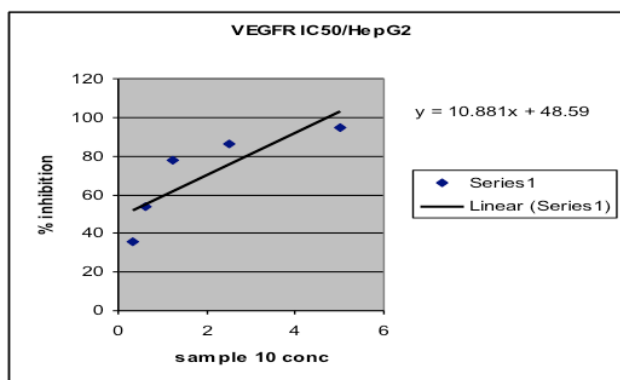
3.2.2 VEGFR-2 inhibition in human liver cancer cell line HepG-2

In a trial to explore the mechanism of action of the most active compounds **5**, **9**, **12** and **13**, they were subjected to *in vitro* evaluation of their VEGFR-2 inhibition activity on HepG2 cell line using the human VEGFR2/KDR ELISA kit and percentage inhibition was calculated and compared with that of doxorubicin. It was carried out at VACSERA, Cairo, Egypt. The inhibition results for the tested compounds are displayed in **Table 2**.

In vitro biological evaluation of compounds **5**, **9**, **12** and **13** as VEGFR-2 inhibitors revealed remarkable inhibition activity in the range of 83.4 to 87.3% compared to doxorubicin which was active as inhibitor by 79.0%. Compound **13** exhibited the most promising activity as VEGFR-2 inhibitor with inhibition percentage of 87.3%.

IC₅₀ value of the most active compound **13** was determined in order to compare its biological activity with known marketed VEGFR-2 inhibitors using the human VEGFR2/KDR ELISA kit. Five serial dilutions were prepared and measured to construct a standard curve. From linear regression equation, IC₅₀ value could be calculated. It was found that IC₅₀ value of VEGFR-2 inhibition of compound **13** was 0.13 μM; **Fig (2)**. Many VEGFR-2 inhibitors were approved by FDA to be used for cancer treatment as VandetanibII with IC₅₀ values of 0.4±0.13 μM [38].

Figure 2: Standard curve of compound **13**



3.3. Molecular modeling and docking results

The docking process includes the prediction of ligand conformation and orientation within a targeted binding site, in addition to the possible ligand-protein interactions. In general, docking aims at accurate structural modeling of the new hits and correct prediction of the activity [22]. Vascular endothelial growth factor receptors (VEGFRs) classified into: VEGFR-1(Flt-1), VEGFR-2 (KDR/Flk-1) and VEGFR-3(Flt-4) [39]. Downstream effects of VEGFR-2 activation in the vascular endothelium include cell proliferation, migration, permeability and survival, resulting in vasculogenesis and angiogenesis [12]. So VEGFR-2 inhibitors are very important anticancer agents.

The accurate validation of the docking of the co-crystallized ligand [sunitinib (type I inhibitor) (PDB: 4AGD), sorafenib (type II inhibitor) (PDB: 4ASD) or the co-crystallized ligand 99 (type III inhibitor) (PDB: 3VHK)] should be carried out.

Fig. 3, 4, 5. All docking procedures were attained by MOE (Molecular Operating Environment) software 10.2008 provided by chemical computing group, Canada. Performing molecular docking using (PDB: 4AGD), in which we were testing the ability of the compounds to inhibit VEGFR-2 in its ATP binding site did not succeed as the docking score indicates failure of our compounds to interact with this site.

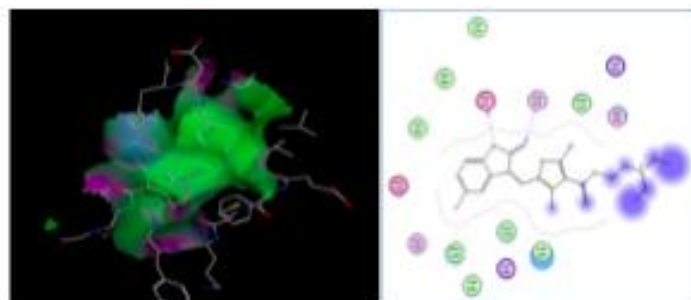


Figure: 3 Docking of the co-crystallized ligand [Sunitinib (Type I inhibitor)]



Figure 4: Docking of the co-crystallized ligand [Sorafenib (Type II inhibitor)]

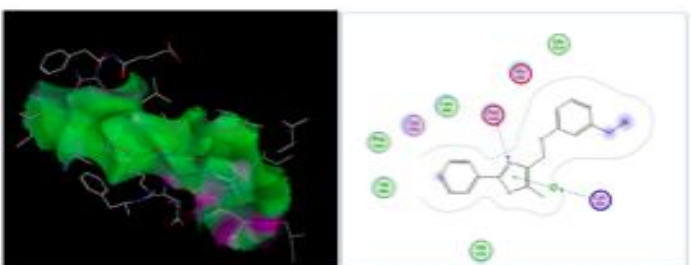


Figure: 5 Docking of the co-crystallized ligand [Ligand 99 (Type III inhibitor)]

Table: 3 Molecular docking scores

compound	(S) Kcal/ mol
5	-12.1220
9	-12.8774
12	-12.8541
13	-13.6740

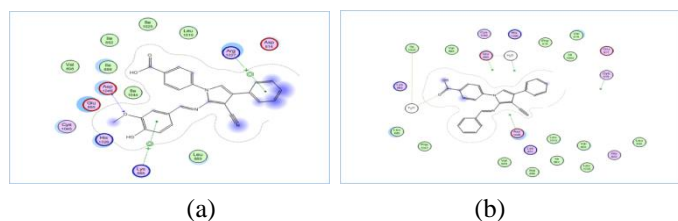


Figure: 6 2D interactions of active compound **13**

(a) with the allosteric binding site (b) as type II inhibitor

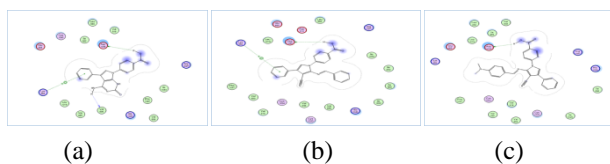


Figure: 7 2D interactions of active compounds with allosteric binding site (a) compound **5** (b) compound **9** (c) compound **12**

The same case was there in our trial to dock the compounds in (PDB: 4ASD) in which type II inhibitor was co-crystallized with VEGFR-2. However, in case of type III inhibitor with PDB ID: 3VHK in a comparable manner to co-crystallized ligand. Ligand 99 (the co-crystallized ligand) was fit on the active site of VEGFR-2 with $S = -12.4340$ Kcal/mol and $rsmd = 0.9272$. The molecular docking scores of the most active four compounds are shown in Table 3. From the table, it could be realized that, all compounds showed a good energy score compared with that of the co-crystallized ligand, especially compound **13** with the least energy score. Compound **13** interacts with the allosteric binding site through hydrogen bonding interaction with Asp 1046, areniumcation interactions with Lys 868 and Arg1027. Also, the high affinity of the compound to the allosteric pocket is attributed to the hydrophobic interactions between the compound and the hydrophobic side chain of amino acids Leu 1019, Ile 1025, Ile 892, Ile 888 and Ile 1044 which line the allosteric pocket. **Fig (6 a,b)**. Also, compounds **5**, **9** and **12** revealed almost the same pattern of interaction with the allosteric binding site. They form hydrogen bonding interaction with Asp 1046 in addition to areniumcation interaction with Lys 868 and the hydrophobic interactions **Fig (7 a,b,c)**

CONCLUSION

From the observed data, it has been noticed that, all the tested compounds reflected promising activity against HepG2 cell line and mild or no activity at all against MCF-7 except compound 18 which revealed moderate activity against MCF-7 ($IC_{50} = 19.2 \pm 0.5 \mu M$) but it showed weak activity against HepG2 ($IC_{50} = 41.2 \pm 1.4 \mu M$). Structure-activity relationship

based on the above results indicated that, substituting the amino pyrrole with mono- and di-acetyl moiety in compounds **6** and **7** with approximately the same IC_{50} values (3.85 ± 0.30 and $3.81 \pm 0.35 \mu M$, respectively) appears more favorable for constructing antitumor compounds than the substitution with ureido moiety in compound **8** ($IC_{50} = 13.59 \pm 1.2 \mu M$). Moreover, aryl group substitution on schiff's base played a controlling role in developing the exhibited pharmacological properties. Substitution with an electron donating group such as dimethylamino **12**, ($IC_{50} = 1.78 \pm 0.10 \mu M$), seems more favorable than the case of an electron withdrawing substituent as a chlorine atom **10**, ($IC_{50} = 12.51 \pm 1.1 \mu M$). In addition, comparing the activity of the compounds bearing the electron donating groups **11** and **12**, it was observed that, the activity increases by increasing the electron donating character of the substitution **11**, ($IC_{50} = 4.79 \pm 0.3 \mu M$) and **12**, ($IC_{50} = 1.78 \pm 0.10 \mu M$). However, the same results were observed in benzamido and phenylsulfonamido series. Compound **24**, bearing electron donating group, has a great activity against HepG2 ($IC_{50} = 7.35 \pm 0.2 \mu M$). While the free carboxylic moiety was converted into amide using sulfonamides in compounds **14-17**, led to abolish the activity against both cell lines. Cyclization to pyrrolopyrimidine derivatives led to good activity especially for the 4-amino, 2-oxo-pyrrolopyrimidine derivative **5** which was the most active compound among this series. However, biological evaluation of compounds **5**, **9**, **12** and **13** as VEGFR-2 inhibitors revealed remarkable inhibition activity in the range of 83.4 to 87.3%. Comparing IC_{50} value as VEGFR-2 inhibitor of compound **13** with vandetanib revealed that compound **13** was approximately 4-folds more potent than vandetanib. Accordingly, compound **13** may be a promising VEGFR-2 inhibitor anticancer agent. In the cytotoxic assay, most active compounds **5,9,12,13** were docked on the active site of VEGFR-2. They tend to be powerful inhibitors through acting as type III Inhibitors. They bind exclusively to the allosteric pocket with good amino acid interactions comparable to the co-crystallized ligand. Compound **13** being the most active *in vitro* VEGFR-2 inhibition assay, shows the least energy score. It binds to the active site through hydrogen bonding interaction, areniumcation interactions and the hydrophobic interactions.

ACKNOWLEDGMENT

The authors would like to express their sincere appreciation to VACSERA, Regional Center for Mycology and Biotechnology,

Al-Azhar University, Faculty of Science, Cairo University and Microanalytical unit, Faculty of Pharmacy, Cairo University.

FINANCIAL ASSISTANCE

Nil

CONFLICT OF INTEREST

The authors declare no conflict of interest

REFERENCES

- [1] Jemal A, Bray F, Center MM, Ferlay J, Ward E, Forman D, Global cancer statistics, CA: A Cancer Journal for Clinicians, 61, 69-90, (2011).
- [2] Ghorab MM, Ceruso M, Alsaid MS, Nissan YM, Arafa RK, Supuran CT, Novel sulfonamides bearing pyrrole and pyrrolopyrimidine moieties as carbonic anhydrase inhibitors: Synthesis, cytotoxic activity and molecular modeling, European Journal of Medicinal Chemistry, 87, 186-196(2014).
- [3] Zwick E, Bange J, Ullrich A, Receptor tyrosine kinase signalling as a target for cancer intervention strategies, Endocrine-Related Cancer, 8 , 161-173(2001).
- [4] Dholakia SP, Patel MM, Patel JS, Role of pyrrolopyrimidine derivatives as anticancer agent: minireview, Indo American Journal of Pharmaceutical Research, 5 , 858-867(2015).
- [5] Mannhold R, Kubinyi H, Folkers G, Klebl B, MüllerG, Hamacher M, Protein Kinases as Drug Targets, John Wiley & Sons, pp. 115-144(2011).
- [6] Motzer RJ, Michaelson MD, Redman BG, Hudes GR, Wilding G, Figlin RA, Ginsberg MS, Kim ST, Baum CM, De Primo SE, Activity of SU11248, a multitargeted inhibitor of vascular endothelial growth factor receptor and platelet-derived growth factor receptor, in patients with metastatic renal cell carcinoma, Journal of Clinical Oncology, 24,16-24(2006).
- [7] Van Oosterom AT, Judson I, Verweij J, Stroobants S, Di Paola ED, Dimitrijevic S, Martens M, Webb A, SciotR, Van Glabbeke M, Safety and efficacy of imatinib (STI571) in metastatic gastrointestinal stromal tumours: a phase I study, The Lancet, 358 , 1421-1423(2001).
- [8] Burris HA, Hurwitz HI, Dees EC, Dowlati A, Blackwell KL, O'Neil B, Marcom PK, Ellis MJ, Overmoyer B, Jones SF, Phase I safety, pharmacokinetics, and clinical activity study of lapatinib (GW572016), a reversible dual inhibitor of epidermal growth factor receptor tyrosine kinases, in heavily pretreated patients with metastatic carcinomas, Journal of Clinical Oncology, 23 , 5305-5313(2005).
- [9] Shepherd FA, Rodrigues Pereira J, Ciuleanu T, Tan EH, Hirsh V, Thongprasert S, Campos D, Maoleekoonpiroj S, Smylie M, Martins R, Erlotinib in previously treated non-small-cell lung cancer, New England Journal of Medicine, 353 , 123-132(2005).
- [10] Ghorab MM, Ragab FA, Heiba HI, Youssef HA, El-Gazzar MG, Synthesis of novel pyrrole and pyrrolo [2,3-d] pyrimidine derivatives bearing sulfonamide moiety for evaluation as anticancer and radiosensitizing agents, Bioorganic & Medicinal Chemistry Letters, 20 ,6316-6320(2010).
- [11] Rock EP, Goodman V, Jiang JX, Mahjoob K, Verbois SL, Morse D, Dagher R, Justice R, Pazdur R, Food and drug administration drug approval summary: sunitinib malate for the treatment of gastrointestinal stromal tumor and advanced renal cell carcinoma, The Oncologist, 12 ,107-113(2007).
- [12] Holmes K, Roberts OL, Thomas AM, Cross MJ, Vascular endothelial growth factor receptor-2: structure, function, intracellular signalling and therapeutic inhibition, Cellular Signalling, 19 ,2003-2012(2007).
- [13] Semenza GL, *N. Engl. J. Med.*, **358**, 2066–7 (2008).
- [14] El Ella DAA, Ghorab MM, Noaman E, Heiba HI, Khalil AI, Molecular modeling study and synthesis of novel pyrrolo [2,3-d] pyrimidines and pyrrolo triazolopyrimidines of expected antitumor and radioprotective activities, Bioorganic & Medicinal Chemistry, 16 ,2391-2402 (2008).
- [15] *Ann Transl Med.* Dec; 2(12): 123 (2014).
- [16] Simard JR, Rauh D, Screening for allosteric kinase inhibitors in high-throughput: A novel fluorescence approach for detecting DFG-out kinase inhibitors, *Screening-Trends in Drug Discovery*, 2-4(2009).
- [17] Sapra S, Sharma K, Bhalla Y, Dhar KL, Chalconoid derived heterocycles as potent bioactive molecules, *Chemical Sciences Journal*, 7:2, 1-8(2016).
- [18] Mohamed MS, Abd El-Hameed RH, Sayed AI, Synthesis strategies and biological value of pyrrole and pyrrolopyrimidine, *Journal of Advanced Pharmacy Research*, 1, 1-24(2017).
- [19] Birnbaum LS, Garfield P, *Journal of American Chemical Society*, 67, 1464 – 1466(1945) .
- [20] Mosmann T, Rapid colorimetric assay for cellular growth and survival: application to proliferation and cytotoxicity

- assays, *Journal of Immunological Methods*, 65, 55-63 (1983).
- [21] Biovendor research and diagnostic products, Human VEGF-R2/KDR ELISA Product Data Sheet
- [22] Kitchen DB, Decornez H, Furr JR, Bajorath J, Docking and scoring in virtual screening for drug discovery: methods and applications, *Nature Reviews Drug Discovery*, 3, 935-949(2004).
- [23] El Ella DAA, Ghorab MM, Noaman E, Heiba HI, Khalil AI, Molecular modeling study and synthesis of novel pyrrolo [2,3-d] pyrimidines and pyrrolo triazolopyrimidines of expected antitumor and radioprotective activities, *Bioorganic & Medicinal Chemistry*, 16 ,2391-2402(2008).
- [24] Ismail M, Ghorab MM, Noaman E, Ammar YA, Heiba HI, Sayed MY, Novel synthesis of pyrrolo [2,3-d] pyrimidines bearing sulfonamide moieties as potential antitumor and radioprotective agents, *Arzneimittel-Forschung*, 56 ,301-308(2005).
- [25] Ghorab MM, Alsaid MS, Nissan YM, Synthesis and molecular docking of some novel anticancer sulfonamides carrying a biologically active pyrrole and pyrrolopyrimidine moieties, *ActaPoloniaePharmaceutica*, 71 ,603(2014).
- [26] Hilmy KMH, Khalifa MM, Hawata MAA, Keshk RMA, El-Torgman AA, Synthesis of new pyrrolo [2,3-d] pyrimidine derivatives as antibacterial and antifungal agents, *European Journal of Medicinal Chemistry*, 45, 5243-5250(2010).
- [27] Mohamed M, El-Domany R, Abd El-Hameed R, Synthesis of certain pyrrole derivatives as antimicro-bial agents, *ActaPharmaceutica*, 59, 145-158(2009).
- [28] Ghorab MM, Ragab FA, Noaman E, Heiba HI, El-Hossary EM, Synthesis of some novel quinolines and pyrimido [4,5-b] quinolines bearing a sulfonamide moiety as potential anticancer and radioprotective agents, *Arzneimittel-Forschung*, 57, 795-803(2006).
- [29] Mohamed MS, Kamel R, Fatahala SS, New condensed pyrroles of potential biological interest: Syntheses and structure-activity relationship studies, *European Journal of Medicinal Chemistry*, 46, 3022-3029(2011).
- [30] Ghorab MM, Heiba HI, Khalil AI, Abou El Ella DA, Noaman E, Computer-based ligand design and synthesis of some new sulfonamides bearing pyrrole or pyrrolopyrimidine moieties having potential antitumor and radioprotective activities, Phosphorus, Sulfur, and Silicon and the Related Elements, 183 ,90-104(2007).
- [31] El-Shaer HM, Abdel-Aziz SAG, Hanafy FI, Ali TES, El-Fauomy AZ, Synthesis, antifungal activity and semi-empirical AM1-MO calculations of some new 4-oxo-4H-chromene derivatives, *European Journal of Chemistry*, 2, 158-162(2011).
- [32] Hranjec M, StarčevićK, PavelićSK, Lučin P, PavelićK, Zamola GK, Synthesis, spectroscopic characterization and antiproliferative evaluation in vitro of novel Schiff bases related to benzimidazoles, *European Journal of Medicinal Chemistry*, 46, 2274-2279(2011).
- [33] Pandeya S, Sriram D, Nath G, De Clercq E, Synthesis, antibacterial, antifungal and anti-HIV activities of Schiff and Mannich bases derived from isatin derivatives and N-[4-(4'-chlorophenyl) thiazol-2-yl] thiosemicarbazide, *European Journal of Pharmaceutical Sciences*, 9, 25-31(1999).
- [34] Chu W, Tu Z, McElveen E, Xu J, Taylor M, Luedtke RR, Mach RH, Synthesis and *in vitro* binding of N-phenyl piperazine analogs as potential dopamine D 3 receptor ligands, *Bioorganic & Medicinal Chemistry*, 13, 77-87(2005).
- [35] Youngs C, Epp A, Craig B, Sallans H, Preparation of long-chain fatty acid chlorides, *Journal of the American Oil Chemists Society*, 34, 107-108 (1957).
- [36] Mohamed M.S, Fathallah SS, Pyrroles and fused pyrroles: synthesis and therapeutic activities, *Mini-Reviews in Organic Chemistry*, 11, 477-507(2014).
- [37] Bennett SM, Nghe NB, Ogilvie KK, Synthesis and antiviral activity of some acyclic and C-acyclic pyrrolo [2,3-d] pyrimidine nucleoside analogs, *Journal of Medicinal Chemistry*, 33 ,2162-2173(1990).
- [38] Brave SR, Odedra R, James NH, Smith NR, Marshall GB, Acheson KL, Baker D, Howard Z, Jackson L, Ratcliffe K, Vandetanib inhibits both VEGFR-2 and EGFR signalling at clinically relevant drug levels in preclinical models of human cancer, *International Journal of Oncology*, 39 ,271-278(2011).
- [39] Hicklin DJ, Ellis LM, Role of the vascular endothelial growth factor pathway in tumor growth and angiogenesis, *Journal of Clinical Oncology*, 23, 1011-1027(2005).